

Dynamic Properties of Cortical Bone Tissue: Izod Tests and Numerical Study

Adel A. Abdel-Wahab¹, Angelo Maligno¹ and Vadim V. Silberschmidt¹

Abstract: Bone is the principal structural component of a skeleton: it assists the load-bearing framework of a living body. Structural integrity of this component is important; understanding of its mechanical behaviour up to failure is necessary for prevention and diagnostic of trauma. In dynamic events such as traumatic falls, involvement in car crash and sports injuries, bone can be exposed to loads exceeding its structural strength and/or fracture toughness. By developing adequate numerical models to predict and describe its deformation and fracture behaviour up to fracture, a detailed study of reasons for, and ways to prevent or treatment methods of, bone fracture could be implemented. This study deals with both experimental analysis and numerical simulations of a cortical bone tissue and its response to dynamic loading. Two areas are covered: impact Izod tests for quantifying a bone's behaviour under impact loading, and a 2-D finite-element model simulating these tests. In the first part the effect of three different parameters - a cortex position, a notch depth and an energy level - on the bones tissue's response to dynamic loading was investigated. Specimens cut from anterior, posterior, medial and lateral cortex position were tested at two different levels of energy for two notch depths. In the second part, a 2D numerical model for the impact Izod test was developed using the Abaqus/Explicit finite-element software. A fully transient formulation employs an initial angular velocity of the hammer together with the real dimensions and material properties of the specimen and the impacting hammer. Three different constitutive material models - linear-elastic, elastic-plastic and viscoelastic - were implemented to compare respective results for impact parameters and fracture force. The obtained experimental results emphasize that bovine femur cortical bone has a nearly uniform fracture energy character with regard to cortex position. The simulation results showed a good agreement of the viscoelastic model with the experimental data.

Keywords: Cortical bone, Izod test, finite-element simulations, dynamic proper-

¹ Wolfson School of Mechanical and Manufacturing Engineering, Loughborough University, Leicestershire, U.K.

ties, impact energy.

1 Introduction

Bone is one of the most challenging natural materials; it is a combination of tropocollagen molecules and nano-hydroxyapatite mineral crystals forming an extremely tough, light-weight, adaptive and multifunctional material (Launey 2010). Since bones provide a structural support to bodies, their mechanical integrity is of great importance. Therefore, degradation of their mechanical properties due to ageing (Zioupos 1998; Nalla 2004) and disease (Giannoudis 2007) or their fracture is an important health concern that has a social and economic impact. In-depth scientific knowledge of the reasons for, and the mechanisms governing, bone fracture helps to plan prevention therapies and/or treatment strategies to inhibit its fracture (Ferreira 2006). Although osteoporosis plays an important role in bone fracture (Melton 1988; Heaney 1993), healthy bones can also fracture due to dynamic events such as traumatic falls, involvement in a car crash or sports injuries. Quantification of bone tissue's mechanical properties can play an important role in a study of the inherent mechanisms of bone fracture. Such data can also underpin analysis of remodelling transformations and develop approaches predicting ultimate bone failure (Ferreira 2006).

Numerous previous studies have been devoted to analysis of quasi-static mechanical properties of a cortical bone tissue, but less attention has been paid to its dynamic mechanical characterization. A small number of papers dealt with dynamic properties of this tissue. For instance, both dynamic and static material properties of a human femur were investigated using a split Hopkinson bar technique and tests with a universal testing machine (Fotios 1990). The average dynamic Young's modulus of 19.9 GPa was found to be 23% greater than that for static loading - 16.2 GPa. Furthermore, there was no significant variation in the magnitude of Poisson's ratio for the two different types of loading. In another study, dynamic tensile material properties of a human pelvic cortical bone were measured at different cortex positions using a high-rate servo-hydraulic Material Testing System (Kemper 2008). Significantly higher values of the ultimate stress, modulus and ultimate strain for horizontally and vertically orientated anterior ilium specimens were obtained for dynamic loading conditions.

In an attempt to investigate a dynamic growth of short cracks, Jan (2006) studied a dynamic behaviour of sub-millimetre microcracks in a cortical bone. It was found that a slow stable crack growth occurred in specimens subjected to static loading conditions. A crack growth direction was dominated by a local fibre orientation in the bone. Short cracks showed periods of rapid growth followed by intervals of crack arrest. Using histological analysis it was shown that crack arrest occurred

due to vascular canals in bone. A strain-controlled propagation was observed with a crack-opening displacement increasing during the period of crack arrest until the local strain was sufficient to overcome those features.

In terms of bone impact characteristics only preliminary data are available (Panagiotopoulos 2005), with a Charpy impact test being used to measure the energy absorbed by strips cut from proximal femur and its relation to age and gender. In a related experimental work, studying cases of fall, *in-vitro* bone toughness was determined as an area under the load-displacement curve obtained in tensile/compression tests using a very low strain rate (Black 1998). However, the load-displacement characteristics of bone are dependent on the rate of the load. Employing an Izod impact tester, Volkan (2008) investigated the absorbed energy and the impact strength of a mandible at different positions. A longitudinal human cortical specimens were tested in a tensile impact tester at a strain rate of 133 s^{-1} (Saha 1976). A marked non-linearity was observed in the stress-strain behaviour including plastic deformation and strain-hardening effects. The mean tensile impact strength and impact energy were $126.3 \pm 33.1 \text{ MPa}$ and $18790 \pm 7355 \text{ J/m}^2$, respectively. Also, statistically significant correlations were found between elastic properties, ultimate stress and impact energy. Moreover, tensile impact strength correlated negatively with an area of secondary osteons in the specimen.

With an increasing number of bone fractures due to factors related to ageing, disease or dynamic events and taking into account the complexity of bone's mechanical behaviour, it becomes more and more important to understand and predict this behaviour using numerical models. The aim of this study is to develop a numerical model to analyse the behaviour of a cortical bone tissue under impact loading. Such a model can be used as a basis for development of more advanced numerical tools capable to predict the behaviour of other bone tissues under arbitrary loading conditions as well as for diseased and osteoporotic bones. Some previous numerical models were developed using a homogenization theory to predict macroscopic behaviour of cortical bone tissue (Crolet 1993; Aoubiza 1996). Several authors, on the other hand, have recently applied cohesive-zone element models to analyze the initiation and propagation of cracks in a cortical bone tissue (Ural 2006; Yang 2006; Cox 2007). Also, a recent study (Morias 2010) demonstrated adequacy of a Double-Cantilever Beam (DCB) test for determining fracture toughness under pure mode I loading of cortical bone by implementing a new data reduction scheme based on specimen compliance. Despite this body of research, experimental and numerical studies of the dynamic behaviour of a cortical bone tissue attracted less attention. Therefore, this study comprises two parts covering experimental and numerical aspects of such analysis.

Even in cases of simple falls bone is subjected to transient loads, therefore, the

amount of energy absorbed is, according to (Panagiotopoulos 2005), perhaps the most valuable result in evaluating bone mechanics. Hence, in our experimental study, Izod tests were performed to assess absorbed energy and fracture force of the bovine cortical bone tissue under impact loading for various levels of applied energy and notch length for specimens from different positions within the bone. The obtained experimental data were also used to validate the developed numerical model. In the numerical study, a hammer-specimen system of the Izod test was modelled using the Abaqus/Explicit finite-element software.

2 Methods and Materials

2.1 Specimen Preparation

Two fresh bovine femora bones, (aged 1.5-2 years), collected from a local butcher were used in this study. The meat was removed, and the bone was chilled before collection. The mid-part of the femur (diaphysis) was extracted using a handsaw. Then, the diaphysis part of the femur was cleaned again to ensure that the outer layer of the cortical bone reached and there was no remaining fat or meat. Since our previous studies of mechanical properties of this bone tissue demonstrated their variability, a transversal cross-section is divided into four main parts (see Fig.1) termed *anterior*, *posterior*, *medial* and *lateral*. Sixteen specimens were cut from these four different cortex positions using a milling machine along the bone axis. Four specimens were used for each position to ensure the reproducibility of the experimental results. All the specimens had the same dimensions (according to ISO 180): 50 mm × 10 mm × 4 mm (length × width × thickness), see Fig. 2a. A 300 μm-deep notch was created perpendicular to the bone axis and along the tangential axis direction in one-half of the specimens using a razor; the notch in the second half was 600 μm. After cutting the specimens, they were ground using a series of grinding papers Standard ANSI grit: 240, 600, and 1200 to make sure that the surface is clean, without any scratches or irregularities. Specimens were stored at room temperature in a 0.9% saline solution until tested.

2.2 Impact Tests

Dynamic impact tests were carried out using a CEAST Resil impactor. In the tests the bottom half of the specimen was fixed firmly in the machine's vice and a knife-edge wedge, (Fig. 2b), was used to define the notch position. The upper half of the specimen was struck by a pendulum hammer with a controlled level of energy. The distance between the notch and the position of hammer strike was standard - 22 mm. In this study a calibrated hammer of 0.334 kg mass and 0.3268 m long was used. The nominal hammer energy of 2 J corresponds to the striking position of

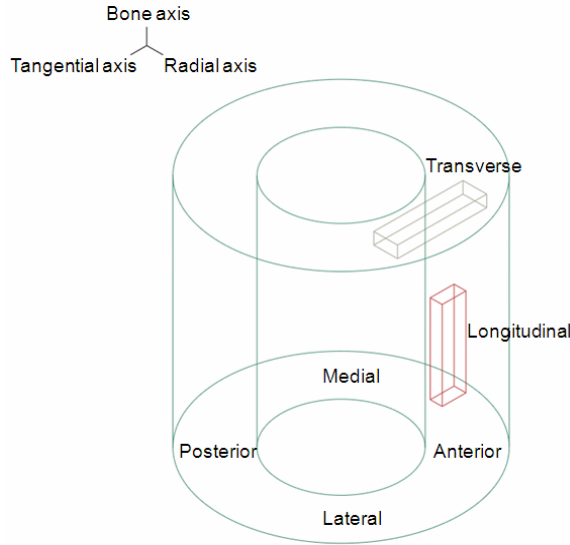


Figure 1: Cortical bone axes and different cortex positions (anterior, posterior, medial and lateral)

150° resulting in an impact velocity of 3.46 m/s. The level of initial energy can be varied by changing the initial angle of the hammer. Two levels of energy were used for each specimen in this study - 0.02 J (non-destructive) and 0.5 J (destructive); they correspond to initial angles of 10° and 58°, respectively. A piezoelectric force transducer was fixed rigidly to the hammer to capture the impact force signal. When the pendulum is released from the pre-defined angle, an impact with the specimen generates a change in the electrical resistance of the piezoelectric sensor that is captured by the data acquisition system - DAS 8000 - connected to the impactor. The measured signal is registered with a sampling frequency of 833 kHz; a 1 kHz filter is used to reduce the noise. The magnitudes of force F and time can be downloaded to a computer; other parameters such as velocity V , displacement d and absorbed energy E can be calculated using the following relationships:

$$V_i = V_{i-1} - \Delta t \left(\frac{F_{i-1} + F_i}{2m} \right) - g, \quad (1)$$

$$d_i = d_{i-1} + \frac{\Delta t}{2} (V_{i-1} + V_i), \quad (2)$$

$$E_i = E_{i-1} + \frac{\Delta t}{2} [(FV)_{i-1} + (FV)_i], \quad (3)$$

where the index i relates to the current time step and $i - 1$ to the previous measurement, with a time difference of Δt ; g is the gravitational acceleration.

The ANOVA test was used for the statistical analysis of the results. It allows testing for differences in the means of different groups. ANOVA tests the null hypothesis that mean values of all the groups are equal. It produces a p-value that is called *level of significance*. A p-value of 0.05 (5%) is generally regarded as sufficiently small to reject the null hypothesis, and it is called the significance level of the test (PASW Statistics 2009).

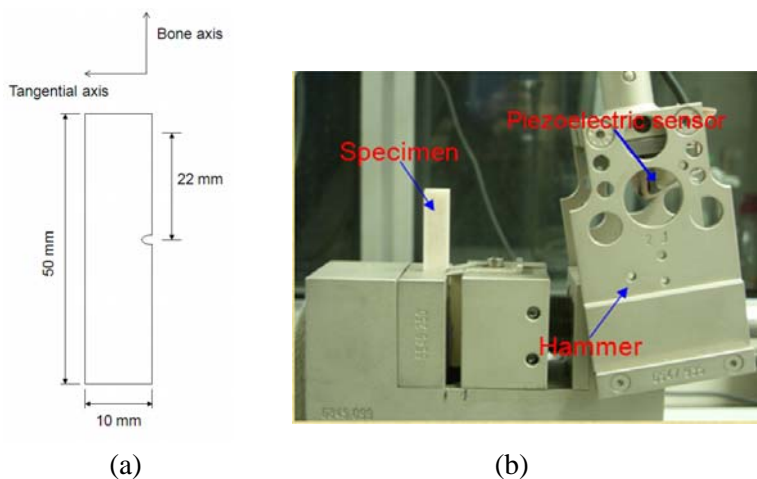


Figure 2: (a) Izod test specimen dimensions, (b) Izod test set-up

2.3 Micro Computed Tomography

A non-destructive characterization technique - X-ray micro computed tomography (μ XCT) - was employed to visualize the three-dimensional microstructure of Izod test specimens before and after a non-destructive impact test. The specimens were scanned using a HMXS CT system to investigate any damage at the microstructural level. The setup of the X-ray power was adjusted to 138 kV and 75 μ A for this test to maximize the signal-to-noise ratio.

Transmitted X-rays resulted in a voxel size in the reconstructed three-dimensional image of 7 μ m. After scanning the notched part of the specimen the studied volume was reconstructed using the CT-Pro2 software. Then the reconstructed volumetric data was post-processed using the VG studio Max 2 software.

3 Numerical Model

The impact tests were simulated with the Abaqus/Explicit finite-element software using at this stage of research a 2-D formulation. The real geometry and masses of the hammer and 300 m notched specimen were used in simulations (see Fig. 3). The elastic material properties for the hammer and the cortical bone tissue used in numerical simulations are given in Tab. 1, while the data on the plastic stress-strain behaviour for bone is given in Tab. 2. The viscous behaviour of bones is introduced into the finite element model in terms of the Prony series expansion of the dimensionless relaxation modulus in the following way:

$$e_R(t) = 1 - \sum_{i=1}^N e_i \left(1 - e^{-t/\tau_i}\right), \quad (4)$$

where e_i and τ_i ($i=1,2, \dots, N$) are material constants; the respective data is provided in Tab. 3. All material properties for cortical bone were obtained in our experiments Abdel-Wahab *et al.* (2010). The following model assumptions were made: (1) plain-stress conditions of the specimen; (2) homogeneous and isotropic material properties for both the specimen and the hammer; (3) frictionless contact between the hammer and the specimen. A special emphasis was on the effect of the type of material's mechanical model on results of simulations: the specimen was presented as an elastic, elastic-plastic and viscoelastic material while the hammer was modelled using an elastic material model due to its significantly higher stiffness.

Table 1: Material properties for finite-element model

Part	Material	Young's modulus (GPa)	Poisson's Ratio	Density (kg/m ³)
Hammer	Steel	210	0.3	7700
Anterior longitudinal	Bone	21.72	0.44	1860

A node on the proximal part of the hammer shown as pivot in Fig. 3b was constrained in x and y directions to simulate its centre of rotation. In simulations the initial position of the hammer was close to the specimen, its angular velocity corresponding to the case with an initial angle of 10° (initial energy of 0.02 J). The specimen's support was modelled as rigid; the degrees of freedom of the specimen's bottom part were constrained (see Figs. 3b and 3c). The linear quadrilateral (CPE4R) and triangular (CPE3) elements were used to mesh the finite-element structure. A total number of 2306 elements and 2433 nodes for the bone specimen and 1964

Table 2: Plastic stress-strain values of anterior longitudinal cortical bone tissue specimens

Plastic strain (mm/mm)	Plastic stress (MPa)
0	99.54
0.00081	110.37
0.00233	120.93
0.00471	125.31
0.00724	128.15
0.00977	130.89
0.01225	134.39
0.01474	137.13
0.017235	140.8

Table 3: Material constants for first three terms of Prony series for anterior longitudinal cortical bone specimens

i	e_i	τ_i
1	-3.43846e-04	1.90787e-03
2	0.10389	0.59147
3	0.53582	43076

elements and 2144 nodes for the hammer were used. It is the current limitations of the XFEM using Abaqus to use only linear elements. The force due to contact pressure between the piezoelectric force sensor and counterpart of the specimen was requested in the history output of the finite-element software Abaqus/Explicit. Based on a convergence study, the stable time increment was 1.46×10^{-6} s.

4 Results

4.1 Results of Izod Tests

The bone fracture behaviour is closely coupled to its hierarchical structure; therefore, the measured fracture parameters depend on the length scale, at which they are evaluated. Moreover, those parameters need to be assessed for a clinically relevant cracking and fracture behaviour, i.e., cracks propagating in a transverse direction, and involve realistic flaw sizes (Koester 2008). Accordingly, in the experimental part of this study, two different initial flaw sizes, 300 μm and 600 μm , were generated in the transverse direction – perpendicular to osteons. A physiologically pertinent flaw sizes were chosen below 600 μm according to (Koester 2008). Also,

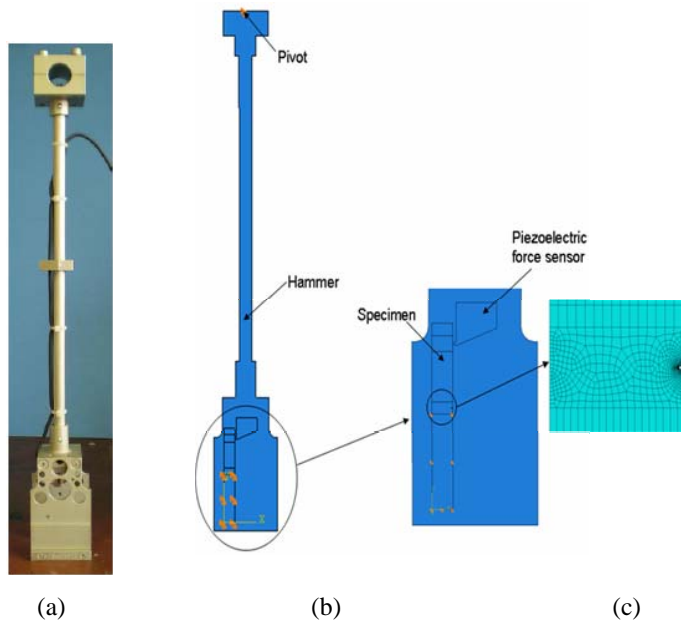


Figure 3: (a) Real hammer. (b) 2-D hammer-specimen finite-element model. (c) Hammer-specimen interaction and mesh around the notch

as it is well known from literature and confirmed in our quasi-static tensile tests, mechanical properties of cortical bone change with cortex positions. Hence, its fracture force and absorbed energy were studied for four different cortex positions using two energy levels – non-destructive and destructive. In the impact Izod test the axial stresses are non-uniformly distributed in a transverse section. Hence, a fracture force parameter is used in place of a fracture stress.

For the specimens subjected to the low energy level – 0.02 J – for both initial notch depths (300 μm or 600 μm), the average recovered energy was approx. 0.016 J for the four cortex positions. The statistical results at that energy level showed no significant difference for specimens from different cortex positions with initial notch depths of 300 μm ($p = 0.774$) or 600 μm ($p = 0.565$). For the higher energy level – 0.5 J – the experimentally measured mean values of fracture force for different cortex positions are shown in Fig. 4. Here, each data set represents the mean value for four specimens and the error bars are the standard deviation (SD) of the measurements. It is seen from Fig. 4 that fracture force of all the cortex positions is lower for specimens with 600 μm initial notch depth compared to those with 300 μm notch, though the difference for medial and lateral specimens of different notch

depths is small - 7% and 4.3%, respectively. Anterior specimens showed the highest fracture force for both notch magnitudes. The medial and posterior positions were characterized by the lowest fracture force values for the initial notches of 300 μm and 600 μm , respectively. The specimens with deeper notches demonstrated lower variability of the obtained data for fracture force. From statistical point of view, based on the use of a one way ANOVA procedure (PASW Statistics 2009), the values of the fracture force express no significant difference for the cortex positions for specimens with 300 μm notches ($p = 0.067$), whereas an increase in the notch depth to 600 μm caused a significant difference ($p = 0.011$). For absorbed energy, Figure 5 shows the mean and standard deviation values for different cortex positions and initial notch depths. It is obvious that – apart from the medial position that has approximately the same average absorbed energy value – specimens with larger initial notches absorb less energy before fracture. The average absorbed energy required to produce fracture appears to be higher at the lateral position, with different magnitudes. However, looking at the spread of the mean absorbed fracture energy for all cortex positions and notch depths, it is apparent that it is within interval from 0.1 J to 0.2 J. The statistical analysis for cortex positions revealed no significant difference of the mean absorbed energy for both notch depths for 300 μm ($p = 0.862$) and for 600 μm ($p = 0.354$). Also, checking the combined effect of both factors – cortex position and notch depth – on the mean absorbed energy no significant difference was demonstrated ($p = 0.642$). Based on these results, bovine femur seems to have cortex position-sensitive fracture force, yet nearly uniform fracture energy.

4.2 Results of Micro-Computed Tomography

A destructive Izod test obviously initiates various damage and fracture mechanisms complicating comparability of dynamic properties' data of cortical bone. Though low-energy non-destructive impacts have caused no visible external damage to specimens or crack initiation in them. The extent of microscopic changes, e.g. in a form of microcracks etc, should be analysed.

Three-dimensional images of the anterior longitudinal bovine cortical bone specimen obtained with X-ray computed tomography before and after non-destructive impact test are shown in Fig. 6.

Analysis of the microstructural features of the specimen demonstrated that the impact at that energy level did not cause any internal damage in the vicinity of the notch and its other parts. This is also confirmed by nearly symmetric shape of the force-time curves of the specimens, see Fig. 7. During the high impact energy test, the specimens were fragmented and it was not possible to obtain the micro XCT images after the test.

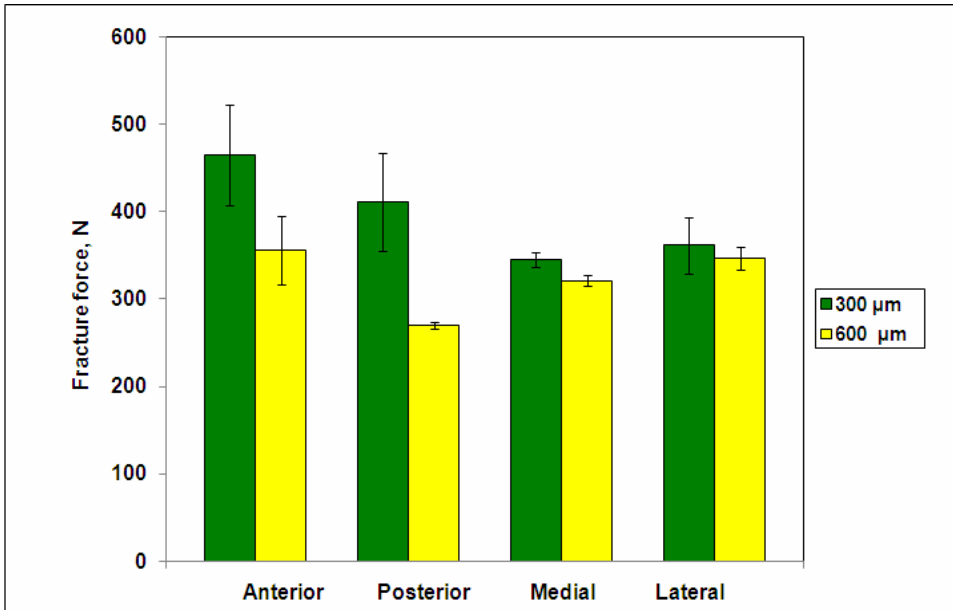


Figure 4: Fracture force of cortical bone specimens from different cortex positions for destructive impact for two different notch depths (error bars represent SD)

4.3 Numerical Results

Based on the experimental results that showed a nearly uniform character of recovered and fracture energy for different cortex positions and notch depths, a numerical model of bone can be introduced only for one notch depth and using properties of one of the four cortex positions. In this study, material data for the anterior part that required the highest fracture force before fracture was chosen to be implemented into the numerical model (see Tabs. 1-3). Several sets of simulations for different material models were performed in this study to analyze their effect on results for the hammer-specimen interaction. A comparison between the experimental data and the results of finite-element simulations for energy level of 0.5 J is shown in Fig. 7.

The obtained results are presented for three different anterior cortical bone material models: linear-elastic, elastic-plastic and viscoelastic. The effect of the type of material model was studied based on our quasi-static tensile test results for the cortical bone tissue that demonstrated elastic-plastic behaviour for a fixed strain rate and sensitivity to strain rate as well as time dependent character. Consequently, an elastic-plastic cortical bone material model (see Tab. 2) was initially implemented

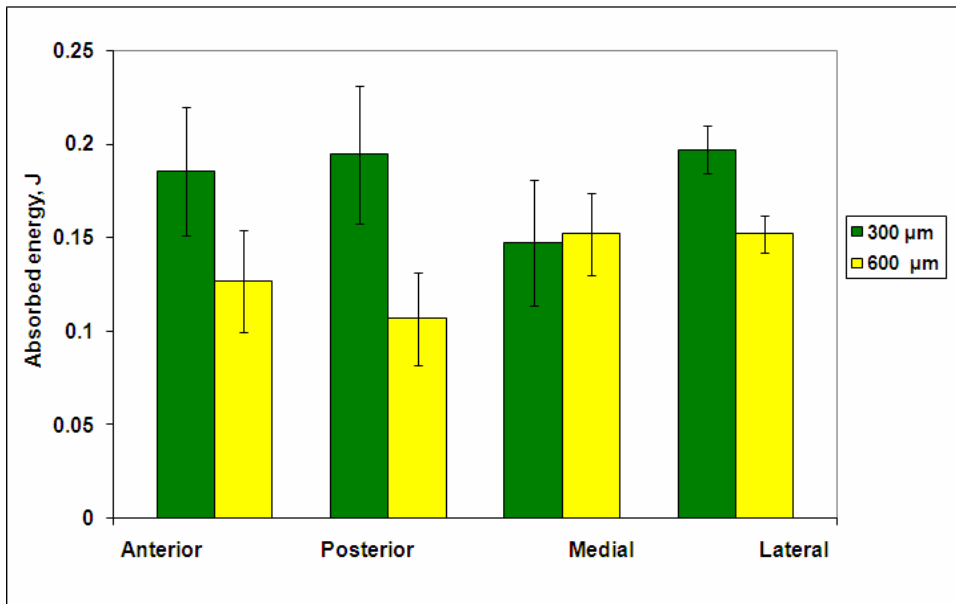


Figure 5: Absorbed fracture energy of cortical bone specimens from different cortex positions for destructive impact for two different notch depths (error bars represent SD)

to ascertain its validity to capture the cortical bone behaviour under impact test. Comparing the results of that model with the obtained experimental data, it was noticed that it underestimated the force magnitude – by 46.7% for its maximum magnitude, indicating its inability to correctly capture the response of the cortical bone tissue under impact load. Moreover, the calculated force peak leads the experimental peak by 0.16 ms (i.e. some 37%).

Then, results of simulations based on the linear-elastic material model were analysed. The introduction of that type of material's behaviour resulted in lower underestimation of the level of force (39.2% lower for the maximum value). Also, similar to elastic-plastic material model, its force peak value leads the experimental peak by 0.16 ms, see Fig. 7. At this point of our analysis, the viscoelastic material model, based on our experimental results (see Tab. 3) was employed; it provided a good agreement with the observed experimental data for the period of interaction between the hammer and specimen in the Izod test. Divergence of numerical and experimental results after the vertical dashed line in Fig. 7, representing the time when the specimen started to fracture, is naturally explained: at that stage of research our models did not employ any fracture criterion that can introduce the

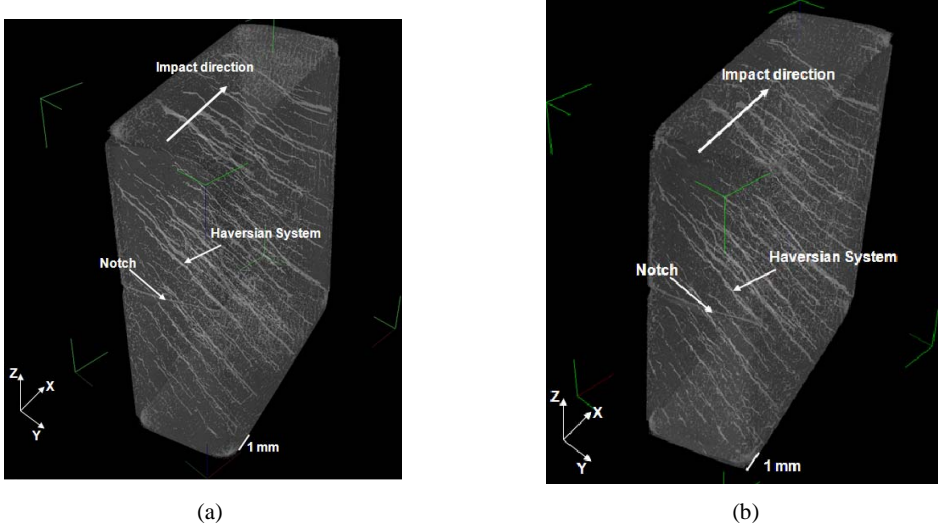


Figure 6: Micro X-ray computed tomography of Izod test specimen before (a) and after (b) non-destructive impact

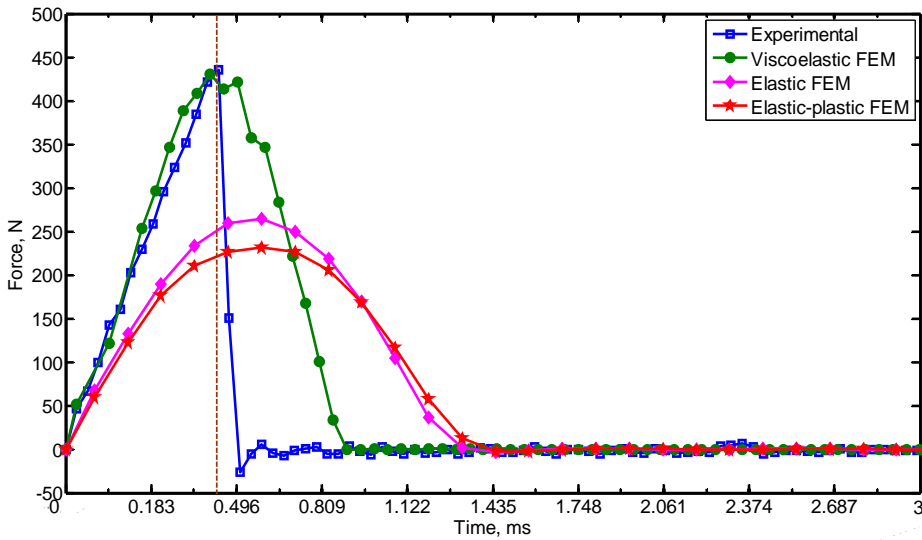


Figure 7: Comparison of experimental and FEM results for anterior cortex position for higher energy level of 0.5 J

specimen's failure behaviour. So, the part of the force-time curve after the peak force exhibits recovery of the stored energy in the specimen, as the hammer was retracting backwards. Thus, the viscoelastic model is capable to present correctly the behaviour of anterior cortical bone under impact loading until the onset of the specimen's fracture. At the next stage of research bone's orthotropic material properties will be incorporated; the effect of microstructural features such as cement lines, lamellae, and pores was accounted by the use of experimental data for the viscoelastic model.

In the case of the low-level impact energy – 0.02 J – the numerical simulations also resulted in three different behaviours for the three different material models as shown in Fig. 8. Here, both linear-elastic and elastic-plastic constitutive models resulted in almost identical behaviour due to a low-level of mechanical excitation. The models based on those two types of material's behaviour underestimated the experimentally obtained peak force magnitude by 8% and 38.5%, respectively, for the lower and upper bounds of the band of experimental data, see Fig. 8. The peak force of the viscoelastic model lies within that band confirming once more the adequacy of the viscoelastic model to simulate the behaviour of cortical bone tissue under impact loading. Employment of the viscoelastic finite-element model leads to a shorter contact time compared to that obtained in simulations with other formulations; it was comparable with the experimentally obtained contact time that was in the range of 1.0 - 1.2 ms.

The next step of our study was to analyse the effect of the constitutive model on the character of evolution of stresses and strains in the bone specimen exposed to dynamic loading. Distributions of the maximum principal stress in the vicinity of the notch tip obtained in the finite-element simulations for impact energy of 0.5 J for three different material models at the force's peak times ($t = 0.43$ ms for viscoelastic model and $t = 0.59$ ms for both linear-elastic and elastic-plastic models) are shown in Fig. 9. It was noticed that both linear-elastic and elastic-plastic models demonstrated a similar character of stress distribution, though with different magnitudes. In contrast, the viscoelastic model had a considerably different character of distribution, with area of higher stresses occupying a significantly larger part of the specimen. For all the models, the highest maximum principal stress magnitude located at the notch's root, starting to decline ahead of the notch and forming nearly symmetric contours in the direct vicinity of the tip. Here, the finite-element model demonstrated the role of the notch as a stress raiser.

As discussed above, linear-elastic and elastic-plastic constitutive models underestimated the maximum force magnitudes. Obviously, the magnitudes of stresses would differ respectively. All the three models produce a very high level of stresses near the notch tip, exceeding the strength of bone. Such high principal stress would

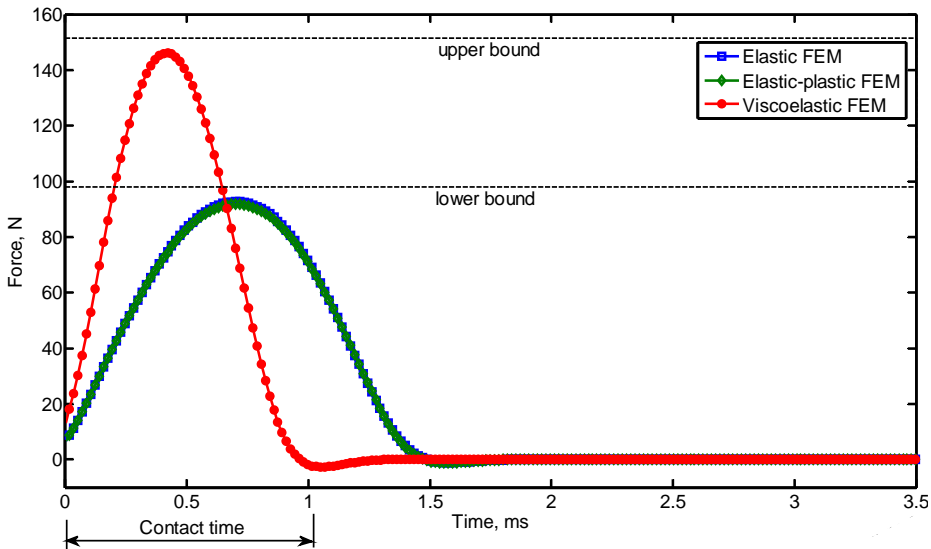


Figure 8: FEM results for anterior cortex position for lower energy level of 0.02 J. horizontal dashed lines represent bounds for experimentally measured values of maximum load

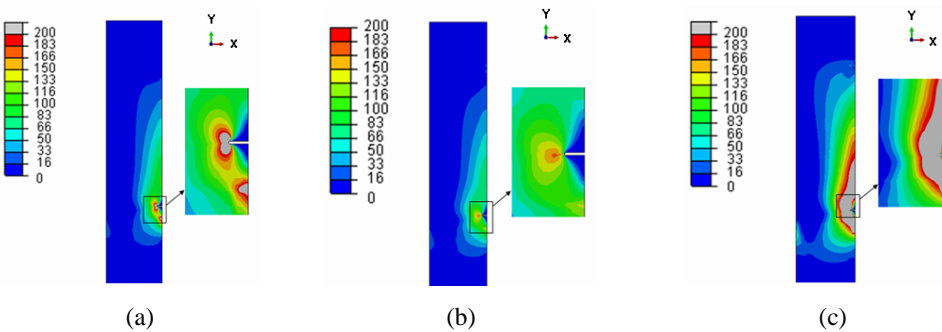


Figure 9: Distribution of maximum principal stress in (MPa) for (a) linear-elastic FEM, (b) elastic-plastic FEM and (c) viscoelastic FEM at peak force time ($t = 0.43$ ms for viscoelastic model and $t = 0.59$ ms for both linear-elastic and elastic-plastic models) for higher energy level of 0.5 J

cause crack initiation not accounted by the models.

An obvious step in analysis is an introduction of the fracture mechanisms. In the case of the cortical tissue an overload results in a crack initiation and propagation. To capture these mechanisms an extended finite-element model (XFEM) was implemented into the viscoelastic model to reproduce the real crack growth in cortical bone tissue under impact. The crack was initiated at the notch's tip where a critical elastic-damage strain driven criterion was met. In this study, the crack was initiated when a critical value of maximum principal strain of 0.3% was reached. The crack started to propagate when a critical value of the strain energy release rate was attained. In our model, the crack propagates in a direction perpendicular to the bone axis; a critical strain energy release rate of 3135 J/m² was used based on results in (Melvin *et al.* 1973). Since the area ahead of the notch tip up to the specimen's neutral axis experience tension, FEM analysis shows that cracks can be initiated perpendicularly to the maximum principal stress's direction. Agreement between the actual crack propagation direction and its simulation were obtained using XFEM, see Fig. 10. Thus, application of XFEM provides a possibility of a quantitative analysis of dynamic crack initiation and propagation; this topic and the respective results will be discussed elsewhere.

The distributions of maximum principal strain for three constitutive models of anterior cortical bone at the force's peak time ($t = 0.43$ ms for viscoelastic model and $t = 0.59$ ms for both linear-elastic and elastic-plastic models) are presented in Fig. 11.

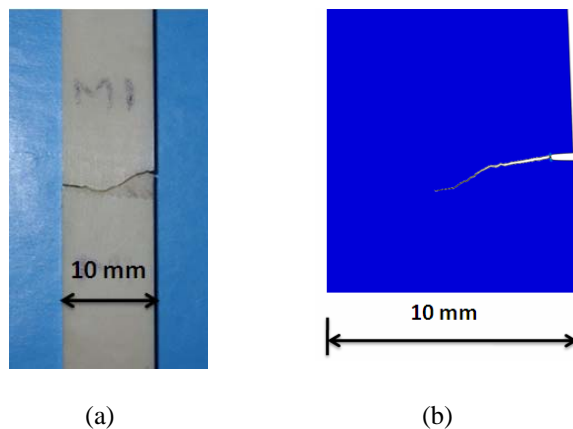


Figure 10: Crack-propagation path for anterior cortical bone Izod test specimen for higher energy level of 0.5 J (a) and results of XFEM simulation (b)

Various material formulations produced different numerical results: the linear-elastic material model had the lowest maximum principal strain levels, while the elastic-plastic had the highest. Obviously, all three distributions have some common features, e.g. strain concentration near the notch tip. Since the attained level of stresses in that area exceeds the yield limit, the plastic formulation resulted in higher principal strain values ahead of the notch. Although the viscoelastic model had the highest principal stress value at the notch's root, its maximum principal strain was lower than that of the elastic-plastic model. This can be naturally explained by short duration of high stresses insufficient for generation of a considerable magnitude of the viscous component of strain. Let's also note that the local shapes and magnitudes of maximum principal strain vary for different material models. In the elastic-plastic model, the area exceeded the yield limit was large and evolving ahead of the notch tip, while it was nearly symmetric and small around the notch tip for both linear-elastic and viscoelastic models.

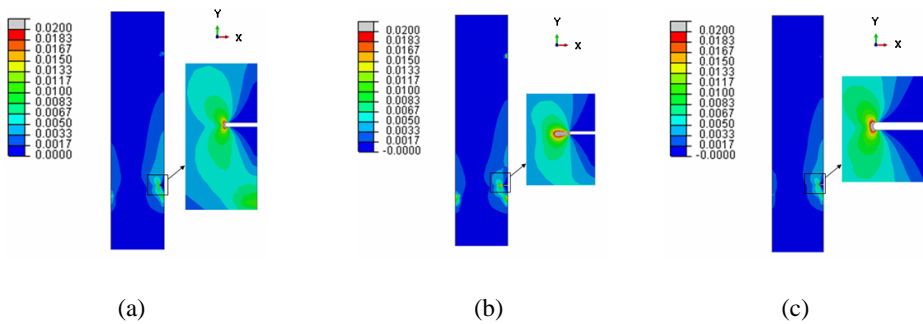


Figure 11: Distribution of maximum principal strain for (a) linear-elastic FEM, (b) elastic-plastic FEM and (c) viscoelastic FEM at peak force time ($t = 0.43$ ms for viscoelastic model and $t = 0.59$ ms for both linear-elastic and elastic-plastic models) for higher energy level of 0.5 J

5 Discussion

The aim of this study was twofold: first, to investigate experimentally the variability of fracture force and fracture energy of bone specimens cut from four different cortex positions and, second, to model numerically the hammer-specimen interaction in the Izod test to analyse the response of bovine cortical bone specimens cut along the femur bone axis. An additional goal was to investigate possible damage at the microstructural scale caused by non-destructive impact energy. Izod test results of specimens cut from different cortex positions showed that at the non-destructive

energy level – 0.02 J – there was no significant difference of the recovered energy for all the positions and for two different notch depths, 300 μm and 600 μm . The reason for this is a nearly perfectly elastic response of material at a low level of energy. No damage or plasticity mechanisms were activated as proved by the symmetry of the force-time curve and was also confirmed by a micro-computed tomography study. On the other hand, when the level of energy increased to a level that caused rupture, it was noticed that there is a significant difference in the fracture force for different cortex positions only for specimens with 600 μm notch, whereas no significant difference was found for a 300 μm notch depth. Therefore, since the threshold of physiologically pertinent flaw sizes is less than 600 μm (according to (Koester 2008)) this means that the diaphysis part of the bovine femur cortical bone has a low variability of the fracture force, in the case of the absence of initial damage/faults. Regarding the fracture energy, no significant difference in the magnitude of that parameter was found for the four cortex positions and notch depths of 300 μm and 600 μm . This is consistent with a study on human cortical femur bone that reported approximately uniform distribution of the relative fracture energy distribution in the diaphysis part (Panagiotopoulos 2005). A study of a section of the tested femora with optical microscopy demonstrated different microstructure, osteonal and primary bone, for various cortex positions. Such microstructural changes are among the reasons for variability of the fracture force; they also affect the fracture energy but its spatial difference was not significant. Most likely, there are different toughening mechanisms for osteonal and primary bones, but the average effect of those mechanisms are nearly the same. These experimental results play an important role in laying the foundation for development of numerical models implementing dynamic analysis of the diaphysis part of the femur. Based on obtained experimental the data only for one quadrant of the femur diaphysis was used in numerical simulations. Additionally, those results are also a better indicator of bone fracture resistance as they are close to fall mechanics (impact injury) as also concluded in another study (Panagiotopoulos 2005).

In this study, applicability of three different material formulations was examined using transient finite-element simulations to investigate the behaviour of cortical bone tissue under impact loading. The simulation results for the viscoelastic constitutive material model showed good agreement with the experimental data. The force's peak magnitude and time as well as the character of force evolution were similar both in experiments and simulations. Hence, these results show the ability of the finite-element model to capture and predict the processes occurring during impact loading before fracture, and highlight the profound role of viscoelasticity of bone in dynamic events such as impact. For the viscoelastic model, a crack propagation path using XFEM implementation represents correctly the main fea-

ture of the real crack's growth process, emphasizing the adequacy of the advanced approach to reproduce the crack path in cortical bone exposed to dynamic loading. Obviously, both initiation and propagation of the crack in a cortical bone tissue would be determined by the local microstructure. Hence, further development of the model by introducing bone's microstructural features can provide an improved tool to model fracture processes in cortical bone tissue under impact loading. It is obvious that to study a bone *in vivo*, embedded in a composite system of muscles and ligaments, it is necessary to develop larger models, directly incorporating other tissues. Still the developed approach is important for elucidating the main deformation and failure mechanisms in bones exposed to dynamic loading. The study of the effects of microstructure on evolution of fracture, e.g. crack propagation, should also start for specific parts and boundary conditions in order to determine interaction with other factors inherent to *in vivo* simulation. This would be the next stage of our research into dynamic behaviour of bone tissue.

6 Conclusions

Experimental tests and various finite-element models were developed and implemented to study the transient dynamic behaviour of cortical bone tissue. The variability of its fracture force and absorbed energy for different cortex positions and notch depths was studied using Izod impact tests. In addition, the applicability of different constitutive material models for analysis of the behaviour of cortical bone tissue under impact loading was also examined. Based on the obtained results from both experimental and numerical studies the following conclusions can be formulated:

- The bovine femoral cortical bone tissue has a nearly uniform character of recovered and fracture energy for different cortex positions and is not sensitive to the notch depth within the physiological pertinent range.
- The studied tissue demonstrates a low variability of the fracture force for specimens with the notch depths of less than 600 μm .
- Impacts with a low energy level of 0.02 J do not activate any damage or plasticity mechanisms in the bovine femoral cortical bone tissue.
- Various 2D numerical models of the hammer-specimen interaction in the Izod test were developed to study the transient dynamic response of cortical bone tissue under impact loading along its longitudinal axis.
- A model based on the Viscoelastic constitutive material description predicts successfully the behaviour of bovine femoral cortical bone up to the onset of

failure under impact loading. Linear-elastic and elastic-plastic constitutive material models underestimate the response of bone specimens to impact loading.

- A combination of viscoelastic constitutive material model and XFEM approach can be used to analyse the onset of cracking and crack propagation under dynamic loading conditions.

Reference

Abdel-Wahab, A.A., Alam, K., Silberschmidt, V.V. (2010): Analysis of anisotropic viscoelastoplastic properties of cortical bone tissues. *J. Mech. Behav. Biomed. Mater.*, doi:10.1016/j.jmbbm.2010.10.001.

Aoubiza, B., Crolet, J.M., Meunier, A. (1996): On the mechanical characterization of compact bone structure using the homogenization theory. *J. Biomech.*, Vol. 29, no. 12, pp. 1539-1547.

Black, J., Hasting, G. (1998): *Handbook of Biomaterial Properties* London, UK, Chapman Hall.

Cox, B. N., Yang, Q. (2007): Cohesive zone models for localization and fracture in bone. *Eng. Fract. Mech.*, Vol. 74, pp. 1079-1092.

Crolet, J. M., Aoubiza, B., Meunier, A. (1993): Compact bone: Numerical simulation of mechanical characteristics. *J. Biomech.*, Vol. 26, no. 6, pp. 677-687.

Ferreira, F., Vaz M.A., Simoes, J.A. (2006): Mechanical properties of bovine cortical bone at high strain rate. *Mater. Charact.*, Vol. 57, pp. 71-79.

Fotios, K., Demetrios, D.R. (1990): Determination of mechanical properties of human femoral cortical bone by the Hopkinson bar stress technique. *J. Biomech.*, Vol. 23, no. 11, pp. 1173-1184.

Giannoudis, P., Tzioupis, C., Almalki, T., Buckley, R., (2007): Fracture healing in osteoporotic fractures: Is it really different? A basic science perspective. *Injury Sci. Basis Fracture Healing: an Update*, Vol. 38, pp. S90-S99.

Heaney, R. P. (1993): Is there a role for bone quality in fragility fractures? *Calcif. Tissue Int.*, Vol. 53, (Suppl 1), pp. 3-5.

Jan, G. H., David, T.T., Clive L. (2006): Dynamic short crack growth in cortical bone. *Technology and Health Care*, Vol. 14: 4-5.

Kemper, A. R., McNally, C., Duma, S.M. (2008): Dynamic tensile material properties of human pelvic cortical bone. *Biomed. Sci. Instrum.*, Vol. 44, pp. 417-418.

Koester, K. J., Ager III, J.W., Ritchie, R.O. (2008): The true toughness of human cortical bone measured with realistically short cracks. *Nat. Mater.*, Vol. 7, pp. 672-

677.

Launey, M. E., Buehler, M.J., Ritchie, R.O. (2010): On the mechanistic origins of toughness in bone. *Annu. Rev. Mater. Res.*, Vol. 40, pp. 9.1-9.29.

Melton, L.J. (1988): *Epidemiology of fracture Osteoporosis, Diagnosis, and Management*. B. L., Riggs, Melton, L.J., New York, Raven Press.

Melvin, J.W., Evans, F.G. (1973): Crack Propagation in Bone. *ASME Biomaterials. Symposium in Detroit MI*.

Morias, J.J.L., de Moura, M.F.S.F., Pereira, F.A.M., Xavier, J., Dourado, N., Dias, M.I.R., Azevedo, J.M.T (2010): The double cantilever beam test applied to mode I fracture characterization of cortical bone tissue. *J. Mech. Behav. Biomed. Mater.*, doi:10.1016/j.jmbbm.2010.04.001.

Nalla, R. K., Kruzic, J.J., Kinney, J.H., Ritchie, R.O. (2004): Effect of ageing on the toughness of human cortical bone: Evaluation by R-curves. *Bone*, Vol. 35, pp. 1240-1246.

Panagiotopoulos, E., kostopoulos, V., Tsantzalis, S., Fortis, A.P., Doulalas, A. (2005): Impact energy absorbtion by specimens from the upper end of the human femur. *Injury*, Vol. 36, pp. 613-617.

PASW Statistics, W. b. P. E. a. C. (2009).

Saha, S., Hayes, W.C. (1976): Tensile impact properties of human compact bone. *J. Biomech.*, Vol. 9, no. 4, pp. 243-244.

Ural, A., Vashishth, D. (2006): Cohesive finite element modelling of age-related toughness loss in human cortical bone. *J. Biomech.*, Vol. 39, pp. 2974-2982.

Volkan, K. (2008): An assessment of impact strength of the mandible. *J. Biomech.* Vol. 41, pp. 3488-3491.

Yang, Q. D., Cox, B.N., Nalla, R.K., Ritchie, R.O. (2006): Re-evaluating the toughness of human cortical bone. *Bone*, Vol. 38, pp. 878-887.

Zioupos, P., Currey, J.D. (1998): Changes in the stiffness, strength, and toughness of human cortical bone with age. *Bone*, Vol. 22, pp. 57-66.

